

Cooperative Cluster Metalation and Ligand Migration in Zirconium Metal–Organic Frameworks

Shuai Yuan, Ying-Pin Chen, Junsheng Qin, Weigang Lu,* Xuan Wang, Qiang Zhang, Mathieu Bosch, Tian-Fu Liu, Xizhen Lian, and Hong-Cai Zhou*

Abstract: Cooperative cluster metalation and ligand migration were performed on a Zr-MOF, leading to the isolation of unique bimetallic MOFs based on decanuclear Zr_6M_4 ($M = Ni, Co$) clusters. The M^{2+} reacts with the μ_3 -OH and terminal H_2O ligands on an 8-connected $[Zr_6O_4(OH)_8(H_2O)_4]$ cluster to form a bimetallic $[Zr_6M_4O_8(OH)_8(H_2O)_8]$ cluster. Along with the metalation of Zr_6 cluster, ligand migration is observed in which a Zr–carboxylate bond dissociates to form a M–carboxylate bond. Single-crystal to single-crystal transformation is realized so that snapshots for cooperative cluster metalation and ligand migration processes are captured by successive single-crystal X-ray structures. In^{3+} was metalated into the same Zr-MOF which showed excellent catalytic activity in the acetaldehyde cyclotrimerization reaction. This work not only provides a powerful tool to functionalize Zr-MOFs with other metals, but also structurally elucidates the formation mechanism of the resulting heterometallic MOFs.

Transition-metal cluster complexes have been widely studied for their structures, bonding interactions, and applications in catalysis and magnetism.^[1] Recently, heterometallic multinuclear clusters have attracted increasing attention owing to the interesting ligand dynamics and synergistic effects between different metal species.^[2] Compared to the conventional metal oxide mixtures, the stoichiometry of metal species in heterometallic clusters can be controlled on the atomic scale. However, when deposited onto porous supports, aggregation of these nanoclusters often occurs at elevated temperatures.^[3] Thus, it is urgent to discover new materials with well-separated nanoclusters and controllable stoichiometry of metal species on the molecular level. In this sense, metal–organic frameworks (MOFs) constructed with isolated metal clusters and organic struts are ideal candidates for the employment of heterometallic clusters.^[4] Divalent-metal-containing MOFs have been extensively studied for their exceptional porosity and potential applications in gas storage/separation, catalysis and magnetics.^[4b,5] However, their practical applications are hampered by their sensitivity to ambient

moisture.^[6] Therefore, researchers in recent years have been concentrating on the development of Zr-MOFs, which tend to possess much greater stability through the strength of Zr–O bonds and high connectivity of Zr_6 clusters.^[7] The exceptional chemical stability of Zr-MOFs has made them a suitable platform for the investigation of various applications.^[8] Yet, the underlying functionality of Zr-MOFs is less diversified as opposed to low-valent-metal based MOFs. First, the open metal sites in many Zr-MOFs are not accessible to guest molecules, which diminishes their potential in gas-storage applications, as open metal sites are deemed to be a significant contributor to the gas adsorption enthalpy.^[9] Second, multiple redox states are responsible for many catalytic properties; the catalytic reactions driven by Zr-MOFs are largely restricted within Lewis acid catalysis because of the redox inert nature of Zr^{4+} .^[10] In addition, the diamagnetic property of Zr^{4+} also limits its magnetic applications.

Efforts have been made to functionalize Zr-MOFs with other transition metals by incorporating the active metal species on the nodes of Zr-MOFs. An intuitive approach is to directly construct a MOF from a bimetallic cluster which contains zirconium as structural support and other transition metals as active sites. The one pot synthesis of bimetallic M-Zr-MOFs ($M = 3d$ metal) has been attempted extensively by us but to no avail. As an alternative approach, bimetallic MOFs can be realized by post-synthetic metal exchange or metalation of Zr_6 cluster. Cohen and co-workers reported a titanium-containing analogue of UiO-66 (Ti-UiO-66) synthesized by post-synthetic metal exchange of Zr^{4+} with Ti^{4+} ,^[11a] which was later on revealed to exhibit photocatalytic activity.^[11b–d] The Hupp group demonstrated that the -OH ligands on the Zr_6 nodes of UiO-66 can be metalated with redox-active V^{5+} ions to produce V-UiO-66 for catalysis.^[12a] Gas-phase atomic layer deposition has also been adopted in a Zr-MOF, Nu-1000, to introduce Zn^{2+} and Al^{3+} to the Zr_6 nodes.^[12b] However, despite all these efforts, it is still an elusive goal to obtain the precise structural information of post-incorporated metal centers because of the disordered distributions and low occupancy of the post-synthetically incorporated metal ions.

Single-crystal X-ray diffraction (SCXRD) is a powerful and ubiquitous technique to definitively elucidate structures at the molecular level.^[13] It has been widely used to determine static structures as well as provide direct evidence of consecutive chemical transformations. Utilizing this technique, Doonan and co-workers have recently been able to solve the precise coordination environments of metals on metallo-linkers in MOFs.^[14] This prompted us to study the cluster transformation during the metalation in a crystalline

[*] S. Yuan, Y.-P. Chen, Dr. J. Qin, Dr. W. Lu, X. Wang, Dr. Q. Zhang, M. Bosch, Dr. T.-F. Liu, X. Lian, Prof. Dr. H.-C. Zhou
Department of Chemistry
Texas A&M University
College Station, TX 77843 (USA)
E-mail: weiganglu@yahoo.com
zhou@chem.tamu.edu
Homepage: <http://www.chem.tamu.edu/rgroup/zhou/>

Supporting information and ORCID(s) from the author(s) for this article are available on the WWW under <http://dx.doi.org/10.1002/anie.201505625>.

Zr-MOF matrix via SCXRD. Herein, we report the synthesis of two bimetallic MOFs by performing post-synthetic cluster metalation on PCN-700, a Zr-MOF with 8-connected $[\text{Zr}_6\text{O}_4(\text{OH})_8(\text{H}_2\text{O})_4]$ clusters. SCXRD unambiguously shows that a $[\text{Zr}_6\text{M}_4\text{O}_8(\text{OH})_8(\text{H}_2\text{O})_8]$ ($\text{M} = \text{Co}, \text{Ni}$) cluster is formed as a result of the reaction between M^{2+} ($\text{M} = \text{Co}, \text{Ni}$) and $\text{OH}^-/\text{H}_2\text{O}$ ligands on the $[\text{Zr}_6\text{O}_4(\text{OH})_8(\text{H}_2\text{O})_4]$ cluster. Interestingly, ligand migration is observed concurrently with cluster metalation, in which the ligand dissociates itself from the vertex zirconium atom and bonds to the post-incorporated metal. Single crystallinity is preserved throughout the process so that the structural transformation is recorded by successive SCXRD measurements. As post-synthetic cluster metalation could occur on Zr_6 clusters with reduced connectivity, we believe that it is a general strategy to synthesize bimetallic MOFs containing isolated heterometallic clusters with well-defined structures and metal contents. We anticipate that cluster metalation will offer broad opportunities for a variety of applications including catalysis, gas adsorption, and magnetics. This work also sheds light on the possible mechanism of the cluster transformation process, which is of great importance for the design of functionalized MOFs with high chemical stability.

A Zr-MOF, PCN-700, was chosen as a scaffold structure to build bimetallic MOFs (Figure 1a).^[15] PCN-700 matches up with four criteria for post-synthetic cluster metalation studies. First, as opposed to the 12-connected Zr-cluster in the UiO series, the $[\text{Zr}_6\text{O}_4(\text{OH})_8(\text{H}_2\text{O})_4]$ cluster in PCN-700 is 8-connected with carboxylate ligands, leaving eight terminal

$-\text{OH}^-/\text{H}_2\text{O}$ ligands poised for post-synthetic metalation (Figure 1c). Second, the reactive terminal $-\text{OH}^-/\text{H}_2\text{O}$ ligands are directly exposed to the channels which facilitates metal ion diffusion and thus the metalation reaction. Third, PCN-700 possesses a certain degree of structural flexibility, which endows the framework with structural adaptability during the metalation. In addition, PCN-700 is robust enough to maintain crystallinity during the metalation under solvothermal conditions, which enables us to employ single-crystal X-ray diffraction (SCXRD) to monitor the transformation process. Overall, the reduced connectivity, accessibility, flexibility, and high stability make PCN-700 an optimal platform for implementing the post-synthetic cluster metalation strategy.

To carry out the post-synthetic cluster metalation, PCN-700 crystals were exposed to a DMF (*N,N*-dimethylformamide) solution of $\text{Ni}(\text{NO}_3)_2$ at 85°C for 48 h. The shape and size of PCN-700 crystals were maintained throughout the modification, indicating a single-crystal to single-crystal transformation rather than dissolution and reformation of the crystals. The resultant crystals, designated as PCN-800-(Ni), were refined in the $P4_2/mmc$ space group. Although it exhibits the identical topology to PCN-700 (Figure 1b), the metal nodes and the ligand conformation have undergone dramatic changes. Each Ni^{2+} reacts with two terminal $-\text{H}_2\text{O}$ ligands and one $\mu_3\text{-OH}$ ligand in a Zr_6 cluster to afford a new Zr_6Ni_4 cluster. Interestingly, a ligand migration is concurrently observed during the cluster metalation which involves the dissociation of Zr-carboxylate bond and formation of Ni-carboxylate bond. As a result, the carboxylate ligand migrates from Zr_6 clusters to the expanded Zr_6Ni_4 clusters and bridges a Ni^{2+} and a Zr^{4+} (Figure 1c,d). Each Ni^{2+} is 6-coordinated with one $\mu_4\text{-O}$, two $\mu_3\text{-OH}$, one terminal $-\text{H}_2\text{O}$, and two O atoms from carboxylates, completing an octahedral geometry. Two kinds of crystallographically independent Zr^{4+} ions exist within the Zr_6Ni_4 cluster. The coordination environments of four equivalent Zr^{4+} ions on the equatorial plane are intact during the cluster metalation and ligand migration, whereas two Zr^{4+} ions at axial positions become 6-coordinated with two $\mu_4\text{-O}$, two $\mu_3\text{-O}$, and two terminal $-\text{H}_2\text{O}$. The Zr–O and Ni–O distances, ranging from 2.03 Å to 2.25 Å and 1.94 Å to 2.07 Å, respectively, fall within the normal range.^[7c,16] In stark contrast to other metal exchanged or metalated Zr-MOFs (i.e. Ti-UiO-66 and V-UiO-66),^[11a,12] PCN-800(Ni) is formed through the cleavage of Zr–carboxylate bonds and generation of Ni–carboxylate bonds. Consequently, PCN-800(Ni) is a fundamentally new structure with well-defined Zr_6Ni_4 clusters. To our knowledge, a bimetallic zirconium-containing MOF with Zr_6M_4 ($\text{M} = \text{transition metal}$) nodes has not been reported before.

Given that PCN-700 could undergo cluster metalation and ligand migration with retention of single crystallinity, we turned our efforts to obtaining SCXRD data for the intermediates during the transformation process. Single crystals of PCN-700 were immersed in a DMF solution of $\text{Ni}(\text{NO}_3)_2$ at 85°C and sampled every 2, 4, 6, 12, and 24 h. The samples were analyzed by single-crystal X-ray diffraction which gave snapshots of the structure transformation process. The SCXRD data clearly reveals a cooperative cluster metalation and ligand migration process. As shown in Fig-

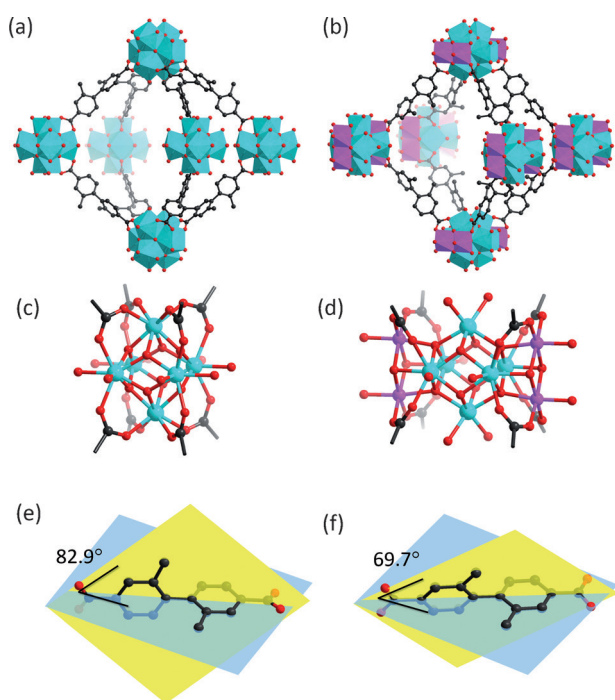


Figure 1. a) The structure of PCN-700; b) the structure of PCN-800-(Ni); c) the Zr_6 cluster in PCN-700; d) the Zr_6Ni_4 cluster in PCN-800(Ni) showing the incorporated Ni and migrated carboxylate ligands; e) the ligand conformation in PCN-700; f) the ligand conformation in PCN-800, see text for details. pink Ni; blue Zr; red O; black C; H atoms are omitted for clarity.

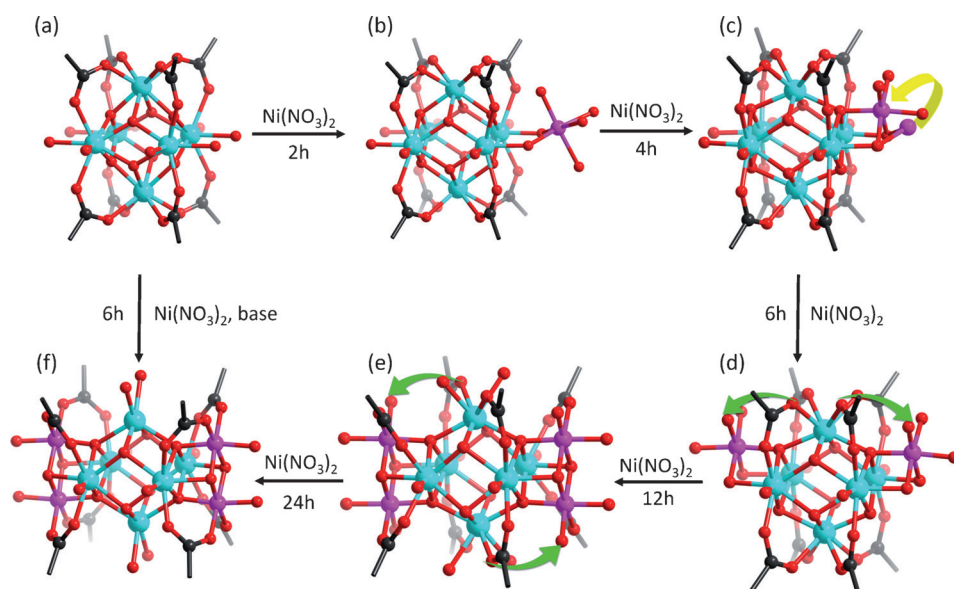


Figure 2. Cluster transformation during the cluster metalation and ligand migration; the yellow arrows illustrate the metal migration and green arrows the ligand migrations.

ure 2b, the Ni^{2+} ions first attach to two terminal $-\text{H}_2\text{O}$. The four disordered Ni^{2+} ions are observed on each Zr_6 clusters with occupancy of 12.5 %, indicating that 0.5 Ni^{2+} is coordinated to each Zr_6 cluster on average. With increased soaking time, the attached Ni^{2+} ion further coordinates with $\mu_3\text{-OH}$ so that each Ni^{2+} is chelated by a $\mu_3\text{-O}$ and two terminal $-\text{OH}$ ligands (Figure 2c). An intermediate is observed in which 20 % of Ni^{2+} is attached to terminal $-\text{OH}$ ligands and 80 % of Ni^{2+} is chelated by a $\mu_3\text{-O}$ and two terminal $-\text{OH}$ ligands (Figure 2c). The ligand migration process occurs along with the cluster metalation. When 1.15 Ni^{2+} is incorporated in each Zr_6 cluster at 6 h, only a negligible amount of ligand migrates. At 12 h, the occupancy of Ni^{2+} reaches 46 % (corresponding to 1.84 Ni^{2+} per Zr_6 cluster) and ligand migration becomes obvious. The site occupancy of Ni^{2+} reaches almost 100 % after 24 h, meanwhile, we are able to observe an intermediate in which half of the ligand migrates. At this stage, the unit cell is doubled compared to PCN-700 because of the decreased symmetry upon ligand migration. Eventually, when the ligand migration completes, the unit cell goes back to its original state. As a result, a MOF based on $[\text{Zr}_6\text{Ni}_4\text{O}_8(\text{OH})_8(\text{H}_2\text{O})_8]$ clusters is generated. The structural transformation of bulk material was characterized by powder X-ray diffraction. It is observed that the peaks at around 7° and 10° gradually split with the incorporation of Ni because of the reduced symmetry, which matches well with the simulations (Figure S3–S8 in the Supporting Information). The bulk materials at each transformation stage have the same composition as single crystals, which was substantiated by energy dispersive X-ray analysis and inductively coupled plasma mass spectrometry (Table S3). It should be noted that the cluster metalation by 3d metal cations have been reported in isolated Zr_6 cluster in which the robust Zr_6 clusters remained during the transformation

whereas the $-\text{OH}$ and carboxylate ligands changed their coordination modes to accommodate the post-incorporated metals.^[16] The resulting heterometallic clusters can also be characterized by SCXRD, but the transformation process remains unclear because of the difficulties in capturing the intermediates.^[16] In our work, however, the crystalline MOF provides a perfect platform to enable us to, for the first time, structurally elucidate the intermediate clusters by SCXRD and therefore garner fundamental insights into the metalation process.

We propose that the deprotonation of terminal $-\text{H}_2\text{O}$ and $\mu_3\text{-OH}$ ligands on Zr_6 clusters is directly correlated to the metal-

ation. According to previous research, $[\text{Zr}_6(\mu_3\text{-O})_4(\mu_3\text{-OH})_4(\text{OH})_4(\text{OH}_2)_4(\text{COO})_8]$ is the preferred form for 8-connected Zr_6 clusters (Figure 3a).^[17] The terminal $-\text{H}_2\text{O}$ is first deprotonated and coordinated to Ni^{2+} ions (Figure 3b). Then, the $\mu_3\text{-OH}$ is deprotonated and coordinated to the same Ni^{2+} , so that this Ni^{2+} is fixed by two $\mu_3\text{-OH}$ and one $\mu_4\text{-O}$ (Figure 3c). Overall, four terminal $-\text{H}_2\text{O}$ ligands are deprotonated to form four $\mu_3\text{-OH}$, meanwhile four $\mu_3\text{-OH}$ ligands are deprotonated into $\mu_4\text{-O}$. The eight negative charges from deprotonation are

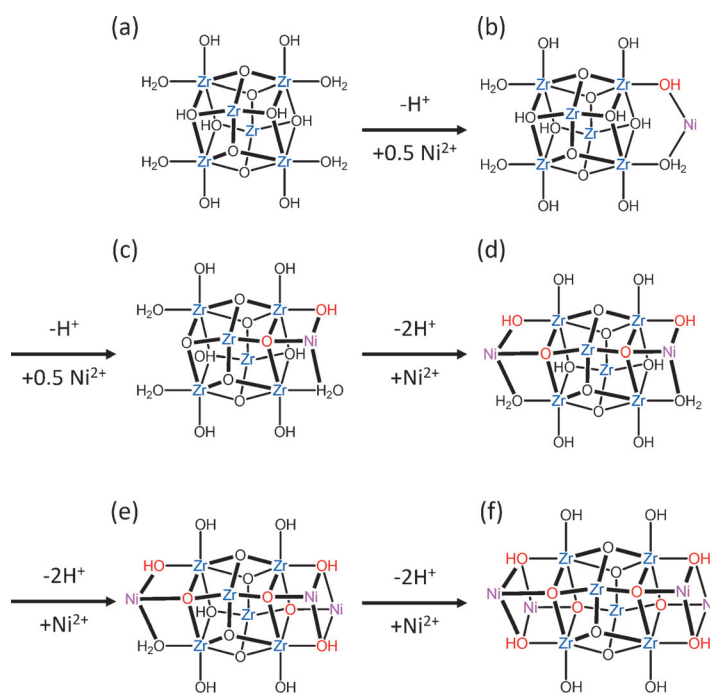


Figure 3. Cluster metalation showing the incorporation of Ni; red indicates the deprotonated ligands.

balanced by four post-incorporated Ni^{2+} ions (Figure 3f). DMF gradually decomposes into dimethyl amine at high temperature in the presence of transition-metal ions, which we believe is responsible for the deprotonation of terminal $-\text{H}_2\text{O}$ and $\mu_3-\text{OH}$ ligands, and thus favors the metalation process. To corroborate our hypothesis, Et_3N or NaOH was added during the post-synthetic cluster metalation in the hope to speed up the deprotonation process of terminal $-\text{H}_2\text{O}$ and $\mu_3-\text{OH}$ ligands, therefore accelerate the metalation process. As expected, with the addition of Et_3N or NaOH to the solution, PCN-800(Ni) can be synthesized in 6 h. In parallel work, the Hupp group very recently also proposed a similar stepwise deprotonation mechanism of cluster metalation, which is supported by computational results and experimental X-ray pair distribution function (PDF) analysis.^[18] Those exhaustive parallel studies largely substantiate our proposed mechanism.

The flexibility of PCN-700 plays an important role in the ligand migration. The conformation of the ligand can undergo dramatic change, allowing the carboxylate group to dissociate from Zr^{4+} and associate with the post-incorporated Ni^{2+} ion. The torsion angle of the linker, defined by two methylphenyl planes, changed from 82.9° in PCN-700 to 69.7° in PCN-800(Ni), as shown in Figure 1e,f. Adaptation of ligand conformation and coordination to meet the coordination environment of inserted metal ions has rarely been reported.^[19] The bulk material maintains its crystallinity after the transformation process as supported by powder X-ray diffraction patterns (Figure S8) and N_2 gas adsorption-desorption isotherms (Figure S13). As a proof-of-concept of the general applicability of this method, $\text{Co}(\text{NO}_3)_2$ was used instead of $\text{Ni}(\text{NO}_3)_2$ under the same conditions, which gave rise to a isostructural bimetallic MOF based on Zr_6Co_4 clusters, designated as PCN-800(Co).

The cluster metalation is a powerful tool to functionalize Zr-MOFs for a variety of applications including chemical catalysis. The acetaldehyde cyclization was selected as a model reaction, which is an industrially attractive process that can lead to many different products (Scheme S2). As InCl_3 is known as a homogeneous catalyst for cyclotrimerization of aldehydes,^[20] we synthesized PCN-800(In) by performing cluster metalation on PCN-700. As a heterogeneous catalyst, PCN-800(In) efficiently catalyze acetaldehyde cyclotrimerization at room temperature under solvent-free condition with conversion of 76% and selectivity up to 99% within 2 h (Figure S16, Table S5). For comparison, no detectable amount of product was observed for pristine PCN-700 under the same conditions.

In summary, we report the synthesis of bimetallic MOFs based on Zr_6M_4 ($\text{M} = \text{Co}, \text{Ni}$) clusters through cooperative cluster metalation and ligand migration. The bimetallic cluster evolution is monitored by successive single-crystal X-ray diffraction analyses, which provide fundamental insights into the metalation process. Given that the cluster metalation could be applied to Zr-MOFs with reduced connectivity, we expect it to be a general and facile strategy to functionalize Zr-MOFs with other metals. In light of the structural diversity and high chemical stability of Zr-MOFs,

this strategy allows for the functionalization of Zr-MOFs for a variety of promising applications.

Acknowledgements

The gas adsorption-desorption studies of this research was supported by the Center for Gas Separations Relevant to Clean Energy Technologies, an Energy Frontier Research Center funded by the U.S. Department of Energy, Office of Science, Office of Basic Energy Sciences under Award Number DE-SC0001015. Structural analyses were supported by Office of Naval Research under Award Number N000141310753. We also acknowledge the financial supports of ARPA-e project funded by the U.S. Department of Energy under Award Number DE-AR0000249 and Welch Foundation under Award Number A-1725. The FE-SEM acquisition of the center was supported by National Science Foundation Grant DBI-0116835, the Vice President for Research Office and the Texas Engineering Experiment Station.

Keywords: cluster metalation · heterometallic MOFs · ligand migration · metal-organic frameworks · zirconium

How to cite: *Angew. Chem. Int. Ed.* **2015**, *54*, 14696–14700
Angew. Chem. **2015**, *127*, 14909–14913

- [1] a) F. A. Cotton, *Rev. Chem. Soc.* **1966**, *20*, 389–401; b) F. A. Cotton, N. F. Curtis, C. B. Harris, B. F. G. Johnson, S. J. Lippard, J. T. Mague, W. R. Robinson, J. S. Wood, *Science* **1964**, *145*, 1305–1307.
- [2] a) P. Buchwalter, J. Rosé, P. Braunstein, *Chem. Rev.* **2015**, *115*, 28–126; b) R. D. Adams, V. Rassolov, Y. O. Wong, *Angew. Chem.* **2014**, *126*, 11186–11189; c) R. D. Adams, B. Captain, *Angew. Chem. Int. Ed.* **2008**, *47*, 252–257; *Angew. Chem.* **2008**, *120*, 258–263.
- [3] O. S. Alexeev, B. C. Gates, *Ind. Eng. Chem. Res.* **2003**, *42*, 1571–1587.
- [4] a) J. Liu, L. Chen, H. Cui, J. Zhang, L. Zhang, C. Y. Su, *Chem. Soc. Rev.* **2014**, *43*, 6011–6061; b) L. Ma, C. Abney, W. Lin, *Chem. Soc. Rev.* **2009**, *38*, 1248–1256; c) J. Lee, O. K. Farha, J. Roberts, K. A. Scheidt, S. T. Nguyen, J. T. Hupp, *Chem. Soc. Rev.* **2009**, *38*, 1450–1459.
- [5] a) H. Furukawa, N. Ko, Y. B. Go, N. Aratani, S. B. Choi, E. Choi, A. Ö. Yazaydin, R. Q. Snurr, M. O’Keeffe, J. Kim, O. M. Yaghi, *Science* **2010**, *329*, 424–428; b) H.-C. Zhou, J. R. Long, O. M. Yaghi, *Chem. Rev.* **2012**, *112*, 673–674; c) J.-R. Li, R. J. Kuppler, H.-C. Zhou, *Chem. Soc. Rev.* **2009**, *38*, 1477–1504; d) T. A. Makal, J. R. Li, W. Lu, H. C. Zhou, *Chem. Soc. Rev.* **2012**, *41*, 7761–7779; e) M. Kurmoo, *Chem. Soc. Rev.* **2009**, *38*, 1353–1379.
- [6] J. A. Greathouse, M. D. Allendorf, *J. Am. Chem. Soc.* **2006**, *128*, 10678–10679.
- [7] a) J. H. Cavka, S. Jakobsen, U. Olsbye, N. Guillou, C. Lamberti, S. Bordiga, K. P. Lillerud, *J. Am. Chem. Soc.* **2008**, *130*, 13850–13851; b) V. Guillerm, F. Ragon, M. Dan-Hardi, T. Devic, M. Vishnuvarthan, B. Campo, A. Vimont, G. Clet, Q. Yang, G. Maurin, G. Férey, A. Vittadini, S. Gross, C. Serre, *Angew. Chem. Int. Ed.* **2012**, *51*, 9267–9271; *Angew. Chem.* **2012**, *124*, 9401–9405; c) H. Furukawa, F. Gándara, Y.-B. Zhang, J. Jiang, W. L. Queen, M. R. Hudson, O. M. Yaghi, *J. Am. Chem. Soc.* **2014**, *136*, 4369–4381.
- [8] a) P. Deria, J. E. Mondloch, E. Tylianakis, P. Ghosh, W. Bury, R. Q. Snurr, J. T. Hupp, O. K. Farha, *J. Am. Chem. Soc.* **2013**,

- 135, 16801–16804; b) D. Feng, Z.-Y. Gu, Y.-P. Chen, J. Park, Z. Wei, Y. Sun, M. Bosch, S. Yuan, H.-C. Zhou, *J. Am. Chem. Soc.* **2014**, *136*, 17714–17717; c) J. Jiang, F. Gándara, Y.-B. Zhang, K. Na, O. M. Yaghi, W. G. Klemperer, *J. Am. Chem. Soc.* **2014**, *136*, 12844–12847; d) Z.-M. Zhang, T. Zhang, C. Wang, Z. Lin, L.-S. Long, W. Lin, *J. Am. Chem. Soc.* **2015**, *137*, 3197–3200.
- [9] H. Wu, Y. S. Chua, V. Krungleviciute, M. Tyagi, P. Chen, T. Yildirim, W. Zhou, *J. Am. Chem. Soc.* **2013**, *135*, 10525–10532.
- [10] F. Vermoortele, B. Bueken, G. Le Bars, B. Van de Voorde, M. Vandichel, K. Houthoofd, A. Vimont, M. Daturi, M. Waroquier, V. Van Speybroeck, C. Kirschhock, D. E. De Vos, *J. Am. Chem. Soc.* **2013**, *135*, 11465–11468.
- [11] a) M. Kim, J. F. Cahill, H. Fei, K. A. Prather, S. M. Cohen, *J. Am. Chem. Soc.* **2012**, *134*, 18082–18088; b) S. J. D. Smith, B. P. Ladewig, A. J. Hill, C. H. Lau, M. R. Hill, *Sci. Rep.* **2015**, *5*, 7823; c) C. Hon Lau, R. Babarao, M. R. Hill, *Chem. Commun.* **2013**, *49*, 3634–3636; d) Y. Lee, S. Kim, J. K. Kang, S. M. Cohen, *Chem. Commun.* **2015**, *51*, 5735–5738.
- [12] a) H. G. T. Nguyen, N. M. Schweitzer, C.-Y. Chang, T. L. Drake, M. C. So, P. C. Stair, O. K. Farha, J. T. Hupp, S. T. Nguyen, *ACS Catal.* **2014**, *4*, 2496–2500; b) J. E. Mondloch, W. Bury, D. Fairen-Jimenez, S. Kwon, E. J. DeMarco, M. H. Weston, A. A. Sarjeant, S. T. Nguyen, P. C. Stair, R. Q. Snurr, O. K. Farha, J. T. Hupp, *J. Am. Chem. Soc.* **2013**, *135*, 10294–10297.
- [13] a) L.-I. Ooi, *Principles of X-ray Crystallography*, Oxford University Press, New York, **2010**; b) G. Sheldrick, *Acta Crystallogr. Sect. A* **2008**, *64*, 112–122.
- [14] W. M. Bloch, A. Burgun, C. J. Coghlan, R. Lee, M. L. Coote, C. J. Doonan, C. J. Sumby, *Nat. Chem.* **2014**, *6*, 906–912.
- [15] S. Yuan, W. Lu, Y.-P. Chen, Q. Zhang, T.-F. Liu, D. Feng, X. Wang, J. Qin, H.-C. Zhou, *J. Am. Chem. Soc.* **2015**, *137*, 3177–3180.
- [16] I. L. Malaestean, M. Speldrich, A. Ellern, S. G. Baca, P. Kögerler, *Dalton Trans.* **2011**, *40*, 331–333.
- [17] N. Planas, J. E. Mondloch, S. Tussupbayev, J. Borycz, L. Gagliardi, J. T. Hupp, O. K. Farha, C. J. Cramer, *J. Phys. Chem. Lett.* **2014**, *5*, 3716–3723.
- [18] a) I. S. Kim, J. Borycz, A. E. Platero-Prats, S. Tussupbayev, T. C. Wang, O. K. Farha, J. T. Hupp, L. Gagliardi, K. W. Chapman, C. J. Cramer, A. B. F. Martinson, *Chem. Mater.* **2015**, *27*, 4772–4778; b) D. Yang, S. O. Odoh, T. C. Wang, O. K. Farha, J. T. Hupp, C. J. Cramer, L. Gagliardi, B. C. Gates, *J. Am. Chem. Soc.* **2015**, *137*, 7391–7396; c) M. H. Beyzavi, N. A. Vermeulen, A. J. Howarth, S. Tussupbayev, A. B. League, N. M. Schweitzer, J. R. Gallagher, A. E. Platero-Prats, N. Hafezi, A. A. Sarjeant, J. T. Miller, K. W. Chapman, J. F. Stoddart, C. J. Cramer, J. T. Hupp, O. K. Farha, *J. Am. Chem. Soc.* **2015**, *137*, 13624–13631.
- [19] J. Tian, L. V. Saraf, B. Schwenzer, S. M. Taylor, E. K. Brechin, J. Liu, S. J. Dalgarno, P. K. Thallapally, *J. Am. Chem. Soc.* **2012**, *134*, 9581–9584.
- [20] E. Elamparuthi, E. Ramesh, R. Raghunathan, *Synth. Commun.* **2005**, *35*, 2801–2804.

Please note: Minor changes have been made to this manuscript since its publication in *Angewandte Chemie* Early View. The Editor.

Received: June 18, 2015

Revised: August 27, 2015

Published online: October 23, 2015